R. & M. No. 2817
(11,148)
A.R.C. Technical Report

MINISTRY OF SUPPLY

AERONAUTICAL RESEARCH COUNCIL
REPORTS AND MEMORANDA

Aileron Reversal and Wing Divergence of Swept Wings

By

E. G. BROADBENT, B.A.,
and
OLA MANSFIELD, B.Sc.

LONDON: HER MAJESTY'S STATIONERY OFFICE
1954
PRICE 7*s* 6*d* NET

Aileron Reversal and Wing Divergence of Swept Wings

By

E. G. BROADBENT, B.A.,

and

OLA MANSFIELD, B.Sc.

COMMUNICATED BY THE PRINCIPAL DIRECTOR OF SCIENTIFIC RESEARCH (AIR), MINISTRY OF SUPPLY

Reports and Memoranda No. 2817*

September, 1947

Summary.—A method of solution for the aileron reversal speed of a swept wing (with emphasis on sweepback) is developed on the lines of strip and semi-rigid theories.

The influence of the following parameters is investigated :—

(*a*) The degree of sweep.
(*b*) Wing torsional and flexural stiffness.
(*c*) Wing plan-form.
(*d*) Aileron plan form.

Families of curves are given for extended variation of these parameters which may be used for the direct estimation of the reversal speed of a given wing by interpolation.

A solution is given for the wing divergence speed of a swept wing.

The general results have been obtained using simple modes of wing deformation but equations are quoted for any given modes of deformation and the adopted modes are compared with the actual deformations produced by the aerodynamic loading for an extreme case. A suggestion is put forward for improving the accuracy of the semi-rigid approach by an iterative method of solution and the flexural mode of distortion is investigated for a particular case.

1. *Introduction.*—Swept wings can produce serious structural problems owing to elastic effects that are unimportant in an unswept wing[1]. Among these problems is the design of a wing for high aileron (or elevon) reversal speed and for adequate rolling power at operational speeds, since loss of aileron power is caused not only by twisting† but also by bending† of the wings. In swept-back wings of conventional layout both the bending and twisting deformations produce changes of aerodynamic incidence that are unfavourable from the point of view of aileron reversal. Some relief from these effects is probably obtained from the distortion of the wing section, the upward bending of the wing producing camber that is concave upwards and therefore tends to counteract the reduction of the incidence.

The present report covers the theoretical consideration of aileron reversal and wing divergence for swept wings with particular emphasis on aileron reversal of swept-back wings and examines the effects of the following parameters :—the degree of sweep, wing stiffness, wing and aileron plan form. The results are presented as families of curves which may be used for the direct estimation of the reversal speed for any given wing.

* R.A.E. Report Structures 9, received 14th January, 1948.

† In the present report the terms bending and flexure refer to bending along the flexural axis, and twisting and torsion refer to rotation about this axis.

It will be clear that quantitative accuracy of the results is limited by the errors of the aerodynamic and elastic derivatives. The inaccuracies of the latter, using semi-rigid theory and simple modes of deformation are well understood[2,3,4,5] and lead to an estimate of the aileron reversal speed of about 85 to 95 per cent of the speed appropriate to the correct elastic deformation. The errors in reversal speed introduced by the aerodynamic assumptions, using strip theory and simple sweep and compressibility corrections, are more uncertain but would not be expected to exceed ± 25 per cent. If the aerodynamic derivatives and elastic deformations for any specific wing were available from experimental or theoretical sources then greater accuracy than the above would be obtainable.

The results given in the families of curves of the variation of the parameters enable a comparison to be made of the aileron reversal speeds of a swept and unswept wing. As a rough approximation for wings of the same plan form and of average stiffness ratio the wing torsional stiffness would have to be increased by 40 per cent to maintain the same reversal speed if the wing were swept back through 45 deg.

The following factors are favourable for increasing the reversal speed of swept-back wings :— high wing stiffnesses in torsion and flexure, sweepback of the flexural axis, high wing taper in plan form, large aileron chord and the use of balance-tabs. The effect of change of wing camber due to wing bending in the case of an average wing is to increase the reversal speed by not more than 5 per cent.

Wing divergence is not liable to be serious for swept-back wings, as the wing bending provides a stabilising effect, but will be serious for a swept-forward wing. The following factors are favourable for increasing the divergence speed of swept-forward wings :—high wing stiffness, especially in flexure, forward position of flexural axis and high wing-taper in plan form.

2. *Aerodynamic Assumptions.*—A diagram of the straight tapered wing considered is shown in Fig. 1.

The aerodynamic assumptions apply to both the semi-rigid treatment (section 3) and the iterative process (Appendix I) and are as follows :—

(*a*) The aerodynamic axis lies along the quarter-chord.

(*b*) The ratio of the aileron chord to the wing chord is constant over the aileron span. (The iterative process (Appendix I) could take account of variations of aileron chord.)

(*c*) The aileron is torsionally rigid.

(*d*) Aerodynamic forces on strips parallel to the aircraft centre-line are expressible in terms of the local chord and incidence change. The latter consists of the components due to wing torsion and the change of incidence due to wing bending.

(*e*) Change of wing camber due to wing bending has in this work been considered separately (section 4) because of the uncertainty relating to this effect. It is assumed that distortions of the aerodynamic section other than those which can be represented as a simple change of camber do not occur.

(*f*) The theoretical incompressible strip-theory coefficients a_1, a_2, and m have been used and assumed constant along the span.

(*g*) Allowance for compressibility can be made by applying the Glauert correction to the reversal speed as given by Figs. 2 to 12. In a specific calculation corrections should be applied to the individual coefficients.

(*h*) Allowance for sweepback is made by reducing the aerodynamic coefficients by $\sqrt{\cos \beta}$. This law of $\sqrt{\cos \beta}$ is not rigidly justifiable on either a theoretical or experimental basis. It was first suggested, so far as the authors are aware, by McKinnon Wood[7] and may be perhaps as much as 20 per cent out.

It is hoped that a more accurate aerodynamic treatment will be developed on the lines of Falkner's approach (R. & M.1910[6]). No detailed thought has yet been given to the application of Falkner's method but it seems that its use would immensely extend the computational labour, particularly of an iterative method. Some refinement could, of course, be obtained without complication by applying simple factors to the strip-theory coefficients, these factors being derived by comparison of strip theory and Falkner's method applied to certain typical wing configurations.

3. *The Semi-rigid Treatment of the Problem.*—The wing shown in Fig. 1 is considered to be built-in at the root and since the present investigation is limited to the evaluation of the reversal speed when the rolling moment and rolling velocity under applied aileron are both zero this assumption is justified. The other elastic assumptions are as follows :—

(*a*) The flexural axis is straight. For generality the flexural axis is assumed to be at a distance e_0c_0 behind the quarter-chord at the wing root and to be at an angle of ε to the aerodynamic sweepback, ε being small compared with β.

(*b*) The flexural mode of distortion is taken to be parabolic*.

(*c*) The torsional mode of distortion is taken to be linear†.

(*d*) The reference section is at the mid-span of the aileron.

In Appendix II the equations are given for general modes of distortion, and a trial of those adopted is made for a particular construction.

3.1. *Derivation of the Equation.*—It is assumed that the aerodynamic forces on a wing strip parallel to the aircraft centre-line may be expressed in terms of the local incidence and chord. The forces on such a strip are given in the form of a lift and a pitching moment (both acting in the vertical plane through the strip) and the latter is resolved into two moments about and along the axis of bending.

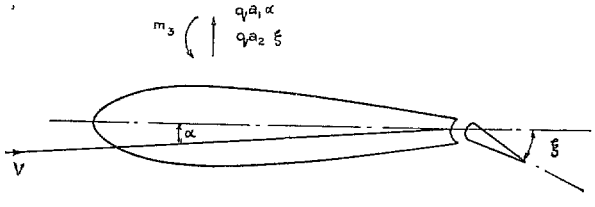

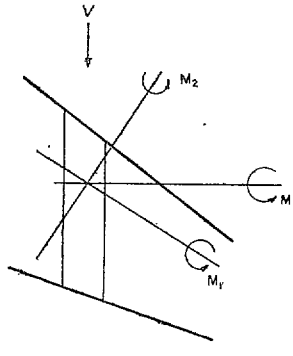

The y' co-ordinate is taken to be along the axis of bending and s' is the value of y' at the tip.

We then have on the application of aileron, for a strip dy ;

$$dL = qc\,dy'\,(a_1\alpha + a_2\xi)\cos\beta \quad .. \quad .. \quad .. \quad .. \quad .. \quad .. \quad .. \quad (1)$$

where L represents the lift force, q the dynamic pressure, c the chord, α the local increment of incidence and ξ the local aileron angle (measured parallel to the centre-line). The coefficients a_1 and a_2 have their usual significance ($a_1 = \partial C_L/\partial\alpha$ and $a_2 = \partial C_L/\partial\xi$) and are assumed constant over the span.

* Some justification of this assumption is given in Appendix I.

† This assumption has been shown to be satisfactory in the case of the unswept wing (R. & M. 2186[4]).

In a similar manner

$$dM = -qc^2\,dy'\,\{m\xi - e(a_2\xi + a_1\alpha)\}\cos\beta \quad .. \quad .. \quad .. \quad .. \quad .. \quad (2)$$

where M denotes the moment about an axis through the flexural centre normal to the aircraft centre-line ; nose-up moments are positive. The distance of the flexural axis aft of the quarter chord is denoted by ec, and $m = -(\partial C_m/\partial\xi)C_L$ constant.

The moment M is now resolved into two components—a moment M_1 about the flexural axis, and a moment M_2 about a line normal to this axis. In addition the equations are written in non-dimensional form, and become

$$dL = qc_0s'(1 - \tau\eta)(a_1\alpha + a_2\xi)\cos\beta\,d\eta \quad .. \quad .. \quad .. \quad .. \quad .. \quad (3)$$

$$\left.\begin{aligned} dM_1 &= -qc_0^2s'(1 - \tau\eta)^2\{m\xi - e(a_2\xi + a_1\alpha)\}\cos^2\beta\,d\eta \\ dM_2 &= -qc_0^2s'(1 - \tau\eta)^2\{m\xi - e(a_2\xi + a_1\alpha)\}\cos\beta\sin\beta\,d\eta \end{aligned}\right\} .. \quad .. \quad (4)$$

Here $\eta = y'/s'$, and the taper τ is defined by

$$c = c_0(1 - \tau\eta)$$

where c_0 is the root chord.

In order to relate the aerodynamic loads given by equations (3) and (4) to the structural distortions, two semi-rigid modes are now chosen. For simplicity the bending mode is taken to be parabolic, and the torsional mode to be linear ; the equations for general modes are given in Appendix II.

Thus if θ denotes the angle of twist (about the flexural axis)

$$\theta = \theta_0(\eta/\eta_0) \quad .. \quad .. \quad .. \quad .. \quad .. \quad .. \quad .. \quad .. \quad .. \quad (5)$$

and if z is the vertical displacement of a point on the flexural axis

$$z = z_0(\eta/\eta_0)^2 \quad .. \quad .. \quad .. \quad .. \quad .. \quad .. \quad .. \quad .. \quad .. \quad (6)$$

where the suffix $_0$ refers to a reference section. By differentiation of equation (6) the mode of bending is obtained in terms of the slope ψ :

$$\psi = \frac{1}{s'}\frac{dz}{d\eta} = \frac{1}{s'}\frac{2z_0}{\eta_0^2}\eta = \psi_0\left(\frac{\eta}{\eta_0}\right). \quad .. \quad .. \quad .. \quad .. \quad .. \quad .. \quad (7)$$

The local incidence is given by

$$\alpha = \theta\cos\beta + \psi\sin\beta, \quad .. \quad .. \quad .. \quad .. \quad .. \quad .. \quad .. \quad (8)$$

and the local aileron angle by

$$\xi = \xi_1 - \theta\cos\beta. \quad .. \quad .. \quad .. \quad .. \quad .. \quad .. \quad .. \quad .. \quad (9)$$

where ξ_1 is a constant equal to $\xi_0 + \theta_0\cos\beta$, and ξ_0 is the value of the aileron angle at the reference section.

The aerodynamic loads given by equations (3) and (4) can now be transferred by the principle of work to equivalent loads at the reference section. The relations are

$$\left.\begin{aligned} dL' &= (\eta/\eta_0)^2\,dL \\ \text{and} \quad dM' &= (\eta/\eta_0)\,dM^* \end{aligned}\right\} .. \quad .. \quad .. \quad .. \quad .. \quad .. \quad (10)$$

After carrying out the substitutions (3), (4), (5), (7), (8) and (9) in the equations (10), and making the further substitution

$$e = \frac{e_0c_0 + s'\eta\varepsilon\sec\beta}{c_0(1 - \tau\eta)} \quad .. \quad .. \quad .. \quad .. \quad .. \quad .. \quad .. \quad .. \quad (11)$$

---

* This equation holds for both components of M since both modes (in terms of the local angle) are linear in y.

he integrations can be effected to give L', M_1' and M_2'. The results of this process may be written

$$\left.\begin{aligned}
L' &= qc_0s' \cos\beta \left\{\frac{a_1A_1}{\eta_0^3}\left(\frac{1}{4}-\frac{\tau}{5}\right)+\frac{a_2\xi_1}{\eta_0^2}\left[\frac{1-\gamma^3}{3}-\frac{\tau(1-\gamma^4)}{4}\right]\right.\\
&\quad \left.-\frac{\theta_0\cos\beta}{\eta_0^3}\left[\frac{1-\gamma^4}{4}-\frac{\tau(1-\gamma^5)}{5}\right]\right\},\\
M_1' &= qc_0^2s' \cos^2\beta \left\{\frac{-m\xi_1}{\eta_0}\left[\frac{1-\gamma^2}{2}-\frac{2\tau}{3}(1-\gamma^3)+\frac{\tau^2}{4}(1-\gamma^4)\right]\right.\\
&\quad +\frac{m\theta_0\cos\beta}{\eta_0^2}\left[\frac{1-\gamma^3}{3}-\frac{2\tau}{4}(1-\gamma^4)+\frac{\tau^2}{5}(1-\gamma^5)\right]+\frac{ea_2\xi_1}{\eta_0}\left[\frac{1-\gamma^2}{2}-\frac{\tau}{3}(1-\gamma^3)\right]\\
&\quad +\left[\frac{1}{\eta_0}\frac{a_2\xi_1s'\varepsilon\sec\beta}{c_0}+\frac{e_0}{\eta_0}(a_1A_1-a_2\theta_0\cos\beta)\right]\left[\frac{1-\gamma^3}{3}-\frac{\tau(1-\gamma^4)}{4}\right]\\
&\quad \left.+\frac{s'\varepsilon\sec\beta}{\eta_0^2c_0}(a_1A_1-a_2\theta_0\cos\beta)\left[\frac{1-\gamma^4}{4}-\frac{\tau}{5}(1-\gamma^5)\right]\right\}.
\end{aligned}\right\} \quad \ldots (12)$$

nd $M_2' = M_1' \tan\beta$;

here $A_1 = \theta_0 \cos\beta + \psi_0 \sin\beta$.

The expressions for L', M_1' and M_2' may now be related to the elastic stiffness by the principle f work. The equations are

$$\left.\begin{aligned}
m_\theta\theta_0 &= M_1'\\
l_\phi\psi_0 &= 4M_2' - 2L'\eta_0s'
\end{aligned}\right\} \quad \ldots \quad (13)$$

It remains to equate the total rolling moment to zero, for the reversal condition

.e., $$\int_0^1 \eta \, dL = 0 \quad \ldots \quad (14)$$

The only unknowns occurring in equations (13) and (14) are q and the ratios ξ_1/θ_0, ψ_0/θ_0. he equations can therefore be solved for q to give the reversal speed.

3.2. *Numerical Solution.*—Solutions have been obtained for a series of variations of the eometric parameters, as shown in Table 1, which also gives the corresponding Figure number.

TABLE 1

Geometry		Corresponding Figure
Taper ratio	$\tau = 0{\cdot}75$	2
Aileron span $(1-\gamma)$	$\gamma = 0{\cdot}6$	
Aileron chord	$E = 0{\cdot}25$	
Aspect ratio	$A = 6$	
Flexural axis	$\varepsilon = 0$, $e_0 = 0$	
Variation of τ $\tau = 0{\cdot}75, 0{\cdot}5, 0{\cdot}25$		2, 4, 3
Variation of γ $\gamma = 0{\cdot}5, 0{\cdot}6, 0{\cdot}7$		7, 2, 8

TABLE 1—*continued*

Geometry	Corresponding Figure
Variation of E $E = 0{\cdot}2, 0{\cdot}25, 0{\cdot}3$	9, 2, 10
Variation of ε $\varepsilon = 0{\cdot}0, 0{\cdot}02, 0{\cdot}04$	2, 11, 12
Variation of A $A = 4, 6, 8$	5, 2, 6

The following values have been assumed for the standard wing :—

Aspect ratio $A = 6$

Wing taper $\tau = 0{\cdot}75$ (*i.e.*, $\frac{\text{Tip chord}}{\text{Root chord}} = 0{\cdot}25$)

Aileron span $\gamma = 0{\cdot}6$ (*i.e.*, $\frac{\text{Aileron span}}{\text{Wing span}} = 0{\cdot}4$)

Aileron chord $E = 0{\cdot}25$ (*i.e.*, $\frac{\text{Aileron chord}}{\text{Wing chord}} = 0{\cdot}25$)

Flexural axis $\begin{cases} e_0 = 0 \\ \varepsilon = 0 \end{cases}$ (*i.e.*, flexural axis at $\frac{1}{4}$-chord)*

Reference section $\eta_0 = 0{\cdot}8$ (*i.e.*, Reference section at mid-aileron position)

Using the above shown standard values the equations for the conditions at reversal for 40 deg sweep reduce to

$$\left.\begin{aligned} M_\theta &= 0{\cdot}127 + 0{\cdot}107p \\ L_\phi &= 0{\cdot}498 + 0{\cdot}593/p \end{aligned}\right\} \quad \ldots\ \ldots\ \ldots\ \ldots\ \ldots\ \ldots\ \ldots \quad (15)$$

where $M_\theta = \dfrac{m_\theta}{qc_m{}^2 S}$, $L_\phi = \dfrac{l_\phi}{qc_m S^2}$, $p = \dfrac{\psi_0}{\theta_0}$ and c_m is the mean chord.

The equations (15) clearly represent a rectangular hyperbola with asymptotes $M_\theta = 0{\cdot}127$ and $L_\phi = 0{\cdot}498$. The stiffnesses are here expressed in non-dimensional form depending on the reversal speed.

The hyperbola appropriate to equation (15) is plotted in Fig. 2 and included in the same graph are curves representing angles of sweep of 0, 30 deg, 35 deg and 45 deg. A series of similar curves covering the variation in the parameters of Table 1 are given in Figs. 3 to 12.

It will be noticed that all the curves possess the same form—that of rectangular hyperbolae except where $\beta = 0$, when, of course, the reversal condition is independent of flexural stiffness. The interpretation of the curves is simply that any condition above and to the right of the curves corresponds to positive control. Thus for positive control to be available at all flying speeds it is necessary that the point (M_θ, L_ϕ) appropriate to the design diving speed should lie above and to the right of the curve referring to the geometry of the particular aircraft concerned.

The practical region for the variation of the non-dimensional parameters is shown in Fig. 2. This region has been obtained statistically, although of necessity the statistics apply chiefly

* This assumption was made to simplify the calculations and is shown later (section 3.3.3) to be justified by the insensitivity of reversal to e_0.

to unswept aircraft. The lower limits shown for M_θ and L_ϕ are appropriate to the design diving speeds (not reversal speeds) of the appropriate aircraft and represent the lowest values given by the survey. There does seem, however, to be a tendency for swept aircraft in the design stage at present to have lower values of L_ϕ. This applies particularly to high speed long range aircraft.

It is not easy to draw detailed inferences from the families of curves about the influence of sweepback, as there is no common assumption which can easily be made for the geometry of wings with different amounts of sweep. The various curves allow direct comparison for wings of the same area and same aspect ratio (except for the case in which aspect ratio is varied, when direct comparison is impossible).

3.3. *Effect of Parameters on Aileron Reversal of Swept-back Wings.*—In Fig. 13 are plotted a series of graphs of the torsional stiffness parameter (M_θ) against various geometric parameters for a selection of three stiffness ratios. The stiffness ratio r is defined by

$$r = \frac{L_\phi}{M_\theta} = \frac{l_\phi}{m_0} \cdot \frac{c}{s} \qquad \ldots \ldots \ldots \ldots \ldots \ldots \ldots \ldots \quad (16)$$

and in practice usually lies in the region of 1·5 to 3. The values of r for which the graphs are plotted, are 1·25, 2·5 and 5, and the results are given for 45 deg sweep and compared with zero sweep. The effects of the various parameters can be examined in turn ; in this case the comparisons are made in terms of M_0, which means that if the stiffness ratio is fixed by other considerations the variation of the required torsional stiffness will be as shown. If both stiffnesses are treated as variables, it does not, of course, follow that high values of r are particularly desirable, for, although they lead to lower values of torsional stiffness, the flexural stiffness itself is higher. In practice, common sense suggests that if the problem of loss of control is to determine both stiffnesses the optimum region (from, say, a weight point of view) in which to work, is that near the axis of the hyperbola. It has been suggested by Lee[8] that quite a sharp weight minimum occurs in this region.

3.3.1. *The effect of sweepback.*—Fig. 13F shows how M_θ depends on β for different values of r, but the effect on design is not so easy to predict, and needs careful interpretation. Indeed it is doubtful whether any definite conclusions can be drawn without actually trying to design to some given specification both with and without sweepback, and comparing the results. If the flexural stiffness is high, for example, sweepback appears to have a beneficial effect on reversal due to the fact that the aerodynamic coefficients are all reduced. But, in the first place the wing area will probably have to be increased due to the fact that $C_{L\max}$ is less for the swept-back wing, and secondly, if the aspect ratio is kept constant, the torsional stiffness will have to be obtained over a greater ratio of length to breadth. On the other hand, the aspect ratio will probably not be kept constant as the wing is swept back. For more normal values of the stiffness ratio the required torsional stiffness increases with sweepback, because of the importance of the bending effect.

3.3.2. *The effect of wing taper.*—Fig. 13A shows that increase of taper is beneficial, though apparently to a somewhat smaller extent for the swept wing than for the unswept wing.

3.3.3. *The effect of sweepback of the flexural axis.*—It has been shown (R. & M. 2186[4]) that for an unswept wing the position of the flexural axis is not very important, and it might be expected that this would also be true for a swept-back wing, as from the point of view of torsion the two are essentially similar. This has been checked by calculation and found to be correct as regards *bodily* movement of the flexural axis. A numerical example may be given for the standard case for zero and 35 deg sweep, and for the flexural axis on the quarter-chord and 10 per cent chord aft of this. The reversal equations are given in Table 2.

TABLE 2

	$e_0 = 0$	$e_0 = 0{\cdot}1$
$\beta = 0^0$	$M_\theta = 0{\cdot}247$	$M_\theta = 0{\cdot}278$
$\beta = 35^0$	$M_\theta = 0{\cdot}150 + 0{\cdot}105\,p$ $L_\phi = 0{\cdot}425 + 0{\cdot}607/p$	$M_\theta = 0{\cdot}169 + 0{\cdot}118\,p$ $L_\phi = 0{\cdot}437 + 0{\cdot}624/p$

When it is remembered that the reversal speed depends on the square root of the values for M_θ and L_ϕ it becomes evident that the parameter e_0 is comparatively unimportant—at least for normal positions of the flexural axis.

On the other hand, relative displacement of the flexural axis along the wing span can have a very pronounced effect—much more so for the swept wing than the unswept wing. This is shown in the graph (Fig. 13B) of M_θ and ε, where the flexural axis though assumed straight is swept back an angle ε relative to the quarter-chord. For instance, in the case $r = 5$, if ε changes from 0 to 0·04 radians, the value of M_θ is halved, or for a given torsional stiffness (m_θ) the reversal speed would be increased from, say, 350 m.p.h. to 500 m.p.h. Of course, this has been worked out for a highly tapered wing so that $\varepsilon = 0{\cdot}04$ is equivalent to a large displacement of the flexural axis towards the wing tip ; at the tip itself the axis is displaced through 60 per cent of the chord. It is probably too much to hope for such a large benefit for a practicable wing construction, but types of construction which tend in the reverse direction (*i.e.*, the flexural axis forward at the tip and aft at the root) should be avoided if possible.

3.3.4. *The effect of aspect ratio.*—Fig. 13A shows that increase of aspect ratio for given stiffness is slightly beneficial, but the problem of providing the stiffness probably more than counterbalances the gain.

3.3.5. *The effect of aileron geometry.*—The effect of span changes considerably with sweepback and stiffness ratio, the change being due to the relative change in importance of the bending deformations. For no sweepback, or for very high flexural stiffness, short ailerons appear to be favourable—though again it must be remembered that the stiffness has to be provided over a greater length of wing ; but for highly swept wings of lower stiffness ratio, the long-span aileron is beneficial. The effect of aileron chord is small in all cases, and is of the same sign as for the unswept wing, namely that increase of chord is slightly beneficial.

4. *Change of Camber on Wing Bending.*—In the preceding analysis it has been tacitly assumed that the aerodynamic section of the wing remained unchanged by the distortion of the wing as a whole. To what extent this approximation is true in practice will depend upon the type of construction adopted, but if the wing is designed with a standard torsion-box and single spar then the wing section in the line of flight will distort as the wing deforms.

This distortion manifests itself as a change of camber of the section, and the magnitude of the change may be estimated from the assumed modes of deformation. As the mode of twist is assumed to be linear this mode will not, of itself, produce any camber change ; on the other hand the parobolic mode of bending will give rise to a constant change of camber over the wing span. Moreover the effect of this camber change is beneficial. For, if an aileron is applied downwards, the wing bends up and acquires camber in the concave sense seen from above which tends to offset the nose-down pitching-moment from the aileron.

The magnitude of the effect has been estimated for a wing swept back at 45 deg, and of constant chord, for three values of the stiffness ratio. The change in the aerodynamic coefficients is based on Glauert's standard two-dimensional theory[9], and the magnitude of the effect in terms of reversal speed was in all cases between 3 and 4 per cent.

5. *Wing Divergence.*—The wing considered is shown in Fig. 1 and the same aerodynamic and elastic assumptions are made as for the semi-rigid treatment of aileron reversal in section 2 with the exception that the flexural axis is at a constant fraction of the chord (e) aft of the quarter-chord, for simplicity. When the wing acquires a positive increment of incidence, the lift forces are increased and the wing bends upwards, and twists nose up. In the absence of bending the twist of the wing would again increase the lift forces and a stable condition or divergence would result, depending on the disturbing air forces and the elastic restoring forces. The upward bending reduces the effective incidence and so for a swept-back wing the bending provides a stabilising effect.

The equations for lift and moment are :—

$$\left.\begin{aligned} dL &= qc_0s'(1 - \tau\eta)a_1\alpha\cos\beta\, d\eta \\ dM &= eqc_0^2s'(1 - \tau\eta)^2a_1\alpha\cos\beta\, d\eta \end{aligned}\right\} \quad \ldots \quad (17)$$

By assuming the modes given by equations (5) and (6) these may be written

$$\left.\begin{aligned} dL &= qc_0s'(1 - \tau\eta)\left(\frac{\eta}{\eta_0}\right)a_1A_1\cos\beta\, d\eta \\ dM &= eqc_0^2s'(1 - \tau\eta)^2\left(\frac{\eta}{\eta_0}\right)a_1A_1\cos\beta\, d\eta \end{aligned}\right\} \quad \ldots \quad (18)$$

The equivalent loads at the reference section corresponding to those for reversal given by the equations (12) are therefore

$$\left.\begin{aligned} L' &= qc_0s'a_1A_1\cos\beta(\tfrac{1}{4} - \tau/5)/\eta_0^3 \\ M_1' &= eqc_0^2s'a_1A_1\cos^2\beta(\tfrac{1}{3} - \tfrac{1}{2}\tau + \tfrac{1}{5}\tau^2)/\eta_0^2 \\ M_2' &= M_1'\tan\beta \end{aligned}\right\} \quad \ldots \quad (19)$$

and the equations of equilibrium are, as before,

$$l_\phi\psi_0 = 4M_2' - 2L'\eta_0s'$$
$$m_\theta\theta_0 = M_1' .$$

For a typical numerical solution, we again resort to the dimensions of Fig. 1 ; choosing $e = 0{\cdot}2$ we then have the equations, for $\beta = 45$ deg.

$$\left.\begin{aligned} M_\theta &= 0{\cdot}212(1 + p) \\ L_\phi &= -2{\cdot}24(1 + 1/p) \end{aligned}\right\} \quad \ldots \quad (20)$$

Again the graph of M_θ and L_ϕ is a rectangular hyperbola, but in this case only a small part of the positive quadrant is enclosed by it. A comparison with the reversal curve is given in Fig. 14 and the comparative unimportance of divergence is quite obvious. The graphs are shaded on the danger side.

The divergence calculations are probably very pessimistic as the assumption of a built-in wing is not justified. If an assumption of constant lift were made, for example, the critical speeds would be much higher. But it would not be very satisfactory for an aircraft to fly at speeds in excess of its ' classical ' divergence speed (*i.e.*, assuming built-in wings) as it would be very susceptible to gusts.

6. *The Effects of Sweep Forward.*—The method of solution of sections 3 and 6 has been applied to a wing similar to that in Fig. 1 but having forward sweep and the results plotted in Fig. 15. The most noticeable feature is that the divergence and aileron reversal curves now appear in the opposite quadrants from the swept-back wing, so that divergence becomes more critical than aileron reversal for the swept-forward wing. In particular the flexural stiffness required to avoid divergence is very high, being double that which would be adequate to prevent aileron reversal on a swept-back wing. Aileron reversal for a swept-forward wing is not very sensitive to flexural stiffness and is avoided entirely with a torsional stiffness appreciably less than would be necessary for an unswept or swept-back wing.

As always for divergence problems it is beneficial to keep the flexural axis as well forward as possible, but it should be noted that whereas an unswept wing with flexural axis at the quarter-chord is stable at all speeds, this is not true for the swept-forward wing, and the flexural stiffness required to prevent divergence can still be very high for appreciable angles of sweep. This stiffness is marked in Fig. 15 (for 45 deg sweep).

7. *Conclusions.*—The conclusions are limited quantitatively by the limits of the aerodynamic treatment but the following qualitative conclusions can be drawn from the results obtained.

Loss of rolling power through structural flexibility is, in general, more serious for sweep-back than for sweep-forward or for no sweep. A possible exception is the case of very high stiffness ratio. The following factors are beneficial and give high aileron reversal speed.

(*a*) High wing-torsional-stiffness.
(*b*) High wing-flexural-stiffness.
(*c*) Sweepback of flexural axis behind aerodynamic axis.
(*d*) High wing taper in plan form.
(*e*) Large aileron chord.
(*f*) The use of balance tabs.

Increase of aileron span is beneficial in reducing the loss of incidence due to bending but detrimental with reference to direct torsion effects and thus the optimum value would depend upon the stiffness ratio and degree of sweep of the particular wing under consideration.

The effect of change of wing camber due to the bending of the wing is small and slightly increases the reversal speed.

Wing divergence is not liable to be serious with swept-back wings but is for swept-forward. The following factors are found to be beneficial and give relatively high divergence speeds for swept-forward wings.

(i) High stiffnesses—especially flexural.
(ii) Well-forward flexural axis.
(iii) High wing taper in plan form.

8. *Further Developments.*—The method used in the present report is to be extended to investigate the effects of wing deformation on the available rolling power at speeds below the aileron reversal speed. For considerations of rolling power, it is incorrect to assume the wing held fixed at the root since the damping terms are important, but the overall effects due to sweep should be similar to those described in the present paper, as the damping can hardly produce any abrupt changes. For the unswept wing it has been shown (R. & M. 2186[4]) that the mode of twist suffers very little change over the speed range up to reversal.

The precise requirements for the control power of future high-speed civil and military aircraft and guided weapons are not clear but since positive control will always be necessary at all flying speeds it seems certain that it will be necessary to predict control power and reversal

speeds accurately for swept wings as in the case of unswept wings. The principle uncertainty (as for all aero-elastic phenomena) is that of the aerodynamic data. This means that much more information is required on the derivatives a_1, a_2, m and the location of the aerodynamic centre with special reference to their dependence on sweep and Mach number. In particular, the reversal speed is very sensitive to the value of m. Data[10,11,12] are becoming available but more are required.

LIST OF PRINCIPAL SYMBOLS

A	Aspect ratio
A_1	Defined by equation (12)
E	Ratio aileron-chord/wing-chord
$F(\eta)$	Flexural mode
L, L'	Lift force and equivalent at reference section
L_ϕ	Non-dimensional stiffness $(l_\phi/qc_m s^2)$
M	Pitching moment
M_1, M_1'	Twisting component of M and equivalent at reference section
M_2, M_2'	Bending component of M and equivalent at reference section
M_θ	Non-dimensional stiffness $m_\theta/qc_m{}^2 s$
P	The flexural rigidity (EI)
a_1, a_2	$\partial C_L/\partial\alpha$, $\partial C_L/\partial\xi$
c, c_0, c_t	Chord, root value and tip value
e, e_0	Position of flexural axis aft of quarter-chord, and value at wing root
$f(\eta)$	Torsional mode
$h(\eta)$	Flexural mode in slope due to distortion in flexure
l_ϕ	Flexural stiffness
m	$-(\partial C_m/\partial\xi)C_L$
m_θ	Torsional stiffness
p	Amplitude ratio $(= \psi_0/\theta_0)$
q	Dynamic pressure $(\frac{1}{2}\rho V^2)$
r	Stiffness ratio $(= cl_\phi/sm_\theta)$
s, s'	Semi-span, and length of wing from root to tip $(= s \sec\beta)$
y, y'	Spanwise co-ordinates perpendicular to centre-line and parallel to flexural axis respectively
z, z_0	Vertical deflection, and value at reference section
α	Incidence
β	Angle of sweep
γ	Inboard end of aileron is γs from centre-line
ε	Angle between flexural axis and quarter-chord line
θ, θ_0	Angle of twist
η, η_0	Non-dimensional spanwise co-ordinate $(= y/s)$
ξ, ξ_1	Aileron angle ; ξ_1 relative to fixed axes and ξ relative to wing
ψ, ψ_0	Angle of bending
τ	Taper $(= 1 - c_t/c_0)$

REFERENCES

No.	Author	Title, etc.
1	A. R. Collar	Some Problems in the Design of Swept-back Wings. A.R.C. 9264. January, 1946. (Unpublished.)
2	D. M. Hirst	Calculation of the Critical Reversal Speed of Wings. R. & M. 1568. September, 1933.
3	Mary Victory	The Calculation of Aileron Reversal Speed. R. & M. 2059. January, 1944.
4	A. R. Collar and E. G. Broadbent ..	The Rolling Power of an Elastic Wing, Part I : Compressibility Effects Absent. R. & M. 2186. October, 1945.
5	E. G. Broadbent and A. R. Collar ..	The Rolling Power of an Elastic Wing, Part II: Compressibility Effects and Results for Supersonic Speeds. R. & M. 2186. October, 1945.
6	V. M. Falkner	The Calculation of Aerodynamic Loading on Surfaces of any Shape. R. & M. 1910. August, 1943.
7	R. McKinnon Wood	Notes on Swept-back Wings for High Speeds. A.R.C. 8806. September, 1945. (Unpublished.)
8	G. H. Lee	Tailless Aircraft Design Problems. *J.R.Ae.S.* February, 1947.
9	H. Glauert	*Aerofoil and Airscrew Theory.* Cambridge University Press. 1926.
10	R. Dickson	The Relationship between the Compressible Flow Round a Swept-back Aerofoil and the Incompressible Flow Round Equivalent Aerofoils. A.R.C. 9986. August, 1946. (Unpublished.)
11	H. M. Lyon and M. Gdaliahu ..	The Estimation of Aerodynamic Loads on Swept-back Wings. A.R.C. 9951. June, 1946. (Unpublished.)
12	C. F. Bethwaite	Preliminary Note on High Speed Tunnel Tests on a Swept-back Wing. A.R.C. 9751. November, 1946. (Unpublished.)
13	A. R. Collar, E. G. Broadbent and Elizabeth Puttick	An Elaboration of the Criterion for Wing Torsional Stiffness. R. & M. 2154. January, 1946.

APPENDIX I

The Flexural Modes of Distortion and Iterative Treatment

A solution of the integral equation for the rolling power of an unswept elastic wing aileron combination has been reported (R. & M. 2186[4,5]) in which the solution was achieved by means of an iterative process applied to a series of chordwise strips along the wing span. This process can be extended fully to cover the case of a swept-back wing subjected to both flexural and torsional deformation. The numerical solution of this more complex problem would, however, be somewhat tedious, and the present investigation is restricted to an artificial case for which the torsional stiffness is assumed infinite. The plan form of the wing considered is shown in Fig. 1.

A.1. *The Integral Equation.*—It is assumed for the purpose of this illustration that the local flexural rigidity (EI) at a section is proportional to the cube of the chord ;

thus $$EI = P = P_0(1 - \tau\eta)^3 \quad . \quad . \quad . \quad . \quad . \quad . \quad . \quad . \quad . \quad . \quad . \quad (A1)$$

Also

$$\xi = \xi_1 = \text{constant}$$

and $$\psi = dz/dy' \quad .$$

The expressions for dM and dL now become

$$\left.\begin{aligned} dM &= -\, qc^2\, dy\, m\xi_1 \\ dL &= qc\, dy\, (a_2\psi \sin\beta + a_2\xi_1) \end{aligned}\right\} \quad . \quad . \quad . \quad . \quad . \quad . \quad . \quad . \quad . \quad (A2)$$

and further the rolling moment due to the strip is

$$dR = qcy\,dy\,(a_1\psi \sin\beta + a_2\xi_1). \qquad \text{(A3)}$$

The total rolling moment is zero, so from (18) we may write

$$\int_0^1 (1 - \tau\eta)\eta(a_1\psi \sin\beta + a_2\xi_1)\,d\eta = 0 \qquad \text{(A4)}$$

which gives a relation for ξ_1.

The bending moment (tip up) at the section y is obtained from equation (A2) as

$$q\int_{y'}^{s'} c^2 m \sin\beta\,\xi_1\,dy_1 + q\int_{y'}^{s'} c(y_1' - y')(a_1\psi \sin\beta + a_2\xi_1)\,dy_1'$$

and this is equal to $-P\dfrac{d\psi}{dy'}$.

The integral equation for ψ is now obtained by integration of this expression. For convenience of solution, we replace ψ by a function $h(\eta)$ such that

$$h(\eta) = \psi/\psi_r$$

where ψ_r is the value of ψ at the reference section. The equation may then be written in non-dimensional form as

$$h(\eta) = \frac{qc_0^2 s^2}{P_0 \cos^2\beta}\int_0^\eta \frac{d\eta}{(1 - \tau\eta)^3}\left\{\int_\eta^1 (1 - \tau\eta_1)^2 A_2 m \sin\beta.\,d\eta_1 + \frac{s}{c_0}\int_\eta^1 (\eta_1 - \eta)(1 - \tau\eta_1)(a_2 A_2 - a_1 h \sin\beta)\sec\beta.\,d\eta_1\right\} \qquad \text{(A5)}$$

where, from equation (A4),

$$A_2 = -\frac{\xi_1}{\psi_r} = \frac{\int_0^1 a_1\eta(1 - \tau\eta)h \sin\beta\,d\eta}{\int_0^1 a_2\eta(1 - \tau\eta)\,d\eta} \qquad \text{(A6)}$$

The equations as written are directly applicable only to the straight tapered wing with a stiffness distribution similar to that assumed. They could, of course, be obtained quite generally in terms of the local values of the chord and the stiffness without affecting the iterative process of solution.

A.2. *Solution of the Equations.*—The iterative method of solving equations of the type of (A5) and (A6) has been described in previous reports[4,5], but in the present case the iterations are a little longer because of the term $(\eta_1 - \eta)$ in equation (A5). The main steps in one iteration are given in Table 3, and briefly explained below.

The first part of the integration from η to 1 (*i.e.*, the part depending on m) is carried out in the usual manner for an assumed mode $h(\eta)$ in column (4) and the result given in column (6). Column (7) gives the product of the terms after the factor $(\eta_2 - \eta)$ in equation (A5). Column (8) represents the bending moment at strip 5 due to the aerodynamic lift on strip 6. It is accordingly 0·0530 (from column 7) multiplied by $(\eta_6 - \eta_5)$. In the same way column 9 represents the bending moment at strip 4 due to the lift outboard of this strip ; it is obtained by summing the bending moments due to each outboard strip, which sum is given at the bottom of the column. Columns (10), (11) and (12) repeat columns (8) and (9) for the bending moments at strips 3, 2 and 1 respectively. The moments on the various strips are arranged vertically in column (13) and after multiplying by s/c_0 are added to those already found from the pitching

moment derivative in column (6) to give column (14). Column (15) represents the final integration, and column (16) the new approximation to the mode. Table 3 gives, in fact, the final iteration, and it can be seen that column (16) repeats column (4) to a sufficient degree of accuracy. The critical value of q is given by

$$0{\cdot}4578qc_0^2s^2 = P_0\cos^2\beta \quad . \quad . . \quad . . \quad . . \quad . . \quad . . \quad . . \quad . . \quad . . \quad \text{(A7)}$$

It will be noted that, by hypothesis, the bending moment at the aircraft centre-line (due to the lift forces) must be zero. This may be seen to be true by extrapolating the numbers in column (13) to the value $\eta = 0$ which is done in Fig. 16. The very fact that the resultant rolling moment is zero may perhaps be taken as an indication that the lift forces alone can have little influence on the reversal speed. That this is not necessarily so is shown by the present example where (partly due to the high aspect ratio and high taper) it will be noted that the factored numbers of column (13) are appreciably greater than the corresponding numbers of column (6). The two are compared in Fig. 16*.

As a more direct comparison of the magnitude of the effect of the lift forces on the reversal speed the iterations have been repeated with the term in the square brackets of equation (A5) made zero. The coefficient corresponding to 0·4578 in equation (A7) was in this case 0·1154.

A.3. *The Approximate Flexural Mode.*—The mode $h(\eta)$ of Table 1 is not the true mode of the wing distortion in flexure, but is a mode of the angular distortion in flexure. The actual mode of vertical deflection is obtained by integration in Table 4.

TABLE 3

General data $a_1 = 5{\cdot}5$, $a_2 = 3{\cdot}37$, $m = 0{\cdot}57$, $\beta = 40°$, $s/c_0 = 2{\cdot}286$, $\gamma = 0{\cdot}6$, $\tau = 0{\cdot}764$

1	2	3	4	5	6	7	8
Strip	$d\eta$	η	$h(\eta)$	Summation for A_2	$\int_{\eta}^{1} \ldots d\eta$	$(1-\tau\eta)$ $\ldots\ldots d\eta_1$	$\int_{\eta_5}^{1} \ldots d\eta_1$
1	0·2	0·1	0·0491	0·0079	0·03332	−0·04184	
2	0·2	0·3	0·2265	0·0912	0·03332	−0·1612	
3	0·2	0·5	0·6123	0·3294	0·03332	−0·3494	
4	0·133	0·666	0·8401	0·3182	0·03332	0·1604	
5	0·133	0·8	1·000	0·3602	0·01639	0·08882	
6	0·133	0·933	1·072	0·3326	0·005785	0·05296	0·007043
				A_2=1·4395			Σ=0·007043

9	10	11	12	13	14	15	16
$\int_{\eta_4}^{1} \ldots d\eta_1$	$\int_{\eta_3}^{1} \ldots d\eta_1$	$\int_{\eta_2}^{1} \ldots d\eta_1$	$\int_{\eta_1}^{1} \ldots d\eta_1$	$\int_{\eta}^{1} \ldots d\eta_1$	(6)+s/c_0(13)	$\int_{0}^{\eta} \ldots d\eta$	$h(\eta)$
				0·02511	0·09072	0·02304	0·0503
			−0·03224	0·06678	0·1860	0·1043	0·2277
		−0·06988	−0·13975	0·07621	0·2075	0·2801	0·6119
	0·02663	0·05872	0·09081	0·02602	0·09279	0·3842	0·8394
0·01190	0·02665	0·04441	0·06218	0·007043	0·03249	0·4578	1·000
0·01414	0·02293	0·03352	0·04411	0·0	0·005785	0·4902	1·071
Σ = 0·02602	Σ = 0·07621	Σ = 0·06678	Σ = 0·02511				

* In the iterations the pitching-moment loads are concentrated at the centres of the strips, but in practice, of course, they only become fully operative at the inboard ends of the strips. This modification has been made in drawing the second curve of Fig. 16.

TABLE 4

1	2	3	4	5
Strip	$h(\eta)$	$\int_0^\eta (h\eta)d\eta$	$F(\eta)$	$1{\cdot}64\eta^{2{\cdot}3}$
1	0·0503	0·0024	0·0067	0·0082
2	0·2277	0·0280	0·0784	0·0877
3	0·6119	0·1120	0·3137	0·3330
4	0·8394	0·2340	0·6555	0·6439
5	1·000	0·3570	1·000	0·9816
6	1·071	0·4930	1·380	1·398

The first four columns of Table 4 are self-explanatory, and in column (4) the true vertical mode is given. The integration of column (3) was performed graphically. An approximate mode of the form

$$F_1(\eta) = A\eta^n$$

has been derived by the method of least squares (*see* for example Ref. 13) and is given in column 5. It may be compared with the true mode of column 4 ; the two modes are also compared in Fig. 17.

It must be emphasised that the work in this section refers only to a wing which is torsionally rigid, and the precise effect of the introduction of the torsional freedom on the flexural mode is not known. However, the writers feel that the result does at least indicate that the assumption of a parabolic mode in flexure is reasonable if no better information is available. The equations for the solution of the reversal problem by semi-rigid theory with general modes are given in Appendix II.

APPENDIX II

Semi-rigid Solution for General Modes

For simplicity we assume the flexural axis to coincide with the quarter-chord. Then the reversal speed is given by solution of the equation*

$$\begin{vmatrix} \frac{m_\theta}{qc_0^2 s} - I_1 \cos^2\beta & , & 0 & , & I_2 \cos\beta \\ I_3 - \frac{c_0}{s} I_4 \sin\beta\cos\beta & , & \frac{l_\phi}{qc_0 s^2 \eta_0^2} + I_5 \tan\beta & , & I_6 \sec\beta + \frac{c_0}{s} I_7 \sin\beta \\ I_8 \cos\beta & , & I_9 \sin\beta & , & I_{10} \end{vmatrix} = 0$$

where the torsion mode is given by

$$\theta = \theta_0 f(\eta)$$

and the mode of flexure by

$$z = z_0 F(\eta)$$

* The equation is developed from the method outlined in the main text.

where θ_0 and z_0 are the values of the twist and vertical displacement respectively at the reference section. The integrals $I_1 \ldots\ldots I_{10}$ are given by

$$I_1 = \int_\gamma^1 m \left(\frac{c}{c_0}\right)^2 f^2 \, d\eta \qquad I_6 = \int_\gamma^1 a_2 \left(\frac{c}{c_0}\right) F \, d\eta$$

$$I_2 = \int_\gamma^1 m \left(\frac{c}{c_0}\right)^2 f \, d\eta \qquad I_7 = \int_\gamma^1 m \left(\frac{c}{c_0}\right)^2 F' \, d\eta$$

$$I_3 = \int_0^1 (a_1 - a_2) \left(\frac{c}{c_0}\right) fF \, d\eta \qquad I_8 = \int_0^1 (a_1 - a_2) \left(\frac{c}{c_0}\right) \eta f \, d\eta$$

$$I_4 = \int_\gamma^1 m \left(\frac{c}{c_0}\right)^2 fF' \, d\eta \qquad I_9 = \int_0^1 a_1 \left(\frac{c}{c_0}\right) \eta F' \, d\eta$$

$$I_5 = \int_0^1 a_1 \left(\frac{c}{c_0}\right) FF' \, d\eta \qquad I_{10} = \int_\gamma^1 a_2 \left(\frac{c}{c_0}\right) \eta \, d\eta$$

Here F' represents $dF/d\eta$.

In the expressions which include the $(a_1 - a_2)$ term it must be remembered that a_2 is zero except over the aileron ; γ denotes the inboard end of the aileron which is assumed to extend to the wing tip.

As a test of the modes assumed in the text, the calculated aerodynamic loading for those modes has been applied to a wing designed with a complete torsion box and approximately constant bending stress under normal lift distribution. Thus for this idealised wing, all the bending strength is effective in torsion ; the skin thickness has been varied linearly from root to tip in such a manner as to satisfy the constant stress requirement. The deformation of this wing under these loads is then shown in Fig. 18 and compared with the assumed algebraic modes.

The agreement achieved for the flexural mode is satisfactory, but that for the torsional mode is not so good. This fact is exaggerated in that the idealised wing provides an extreme case with high taper, and an unbroken torsion box over the very stiff root sections. In most practical cases the mode should be much more linear, as experience has shown it to be for unswept wings[4]. Moreover, since the aerodynamic effect of quite large changes in torsional mode (linear to cubic) have been shown to be small (see Ref. 2) the overall error of the semi-rigid hypothesis should be no greater for a swept wing than for a similar unswept wing.

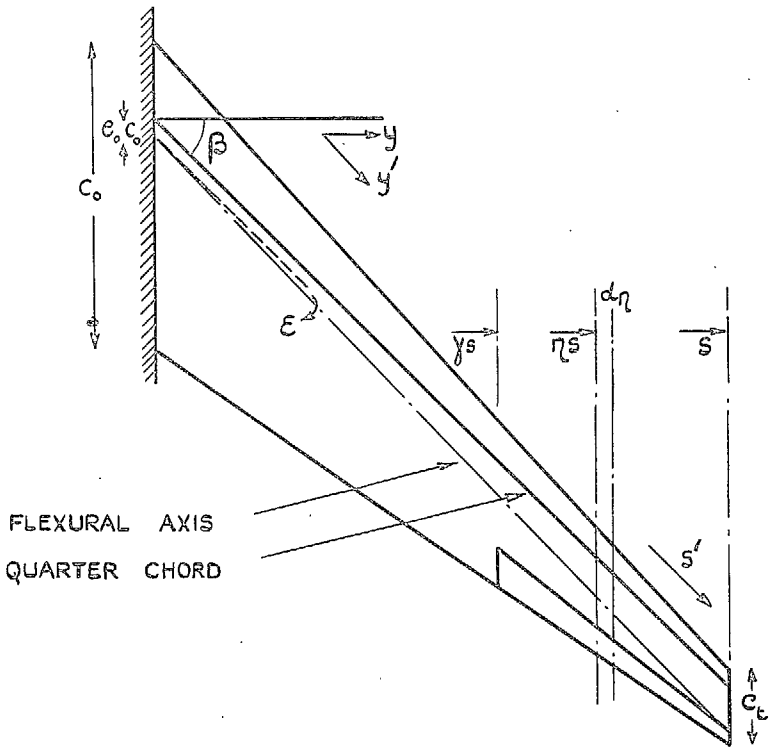

FIG. 1. Diagram of wing considered.

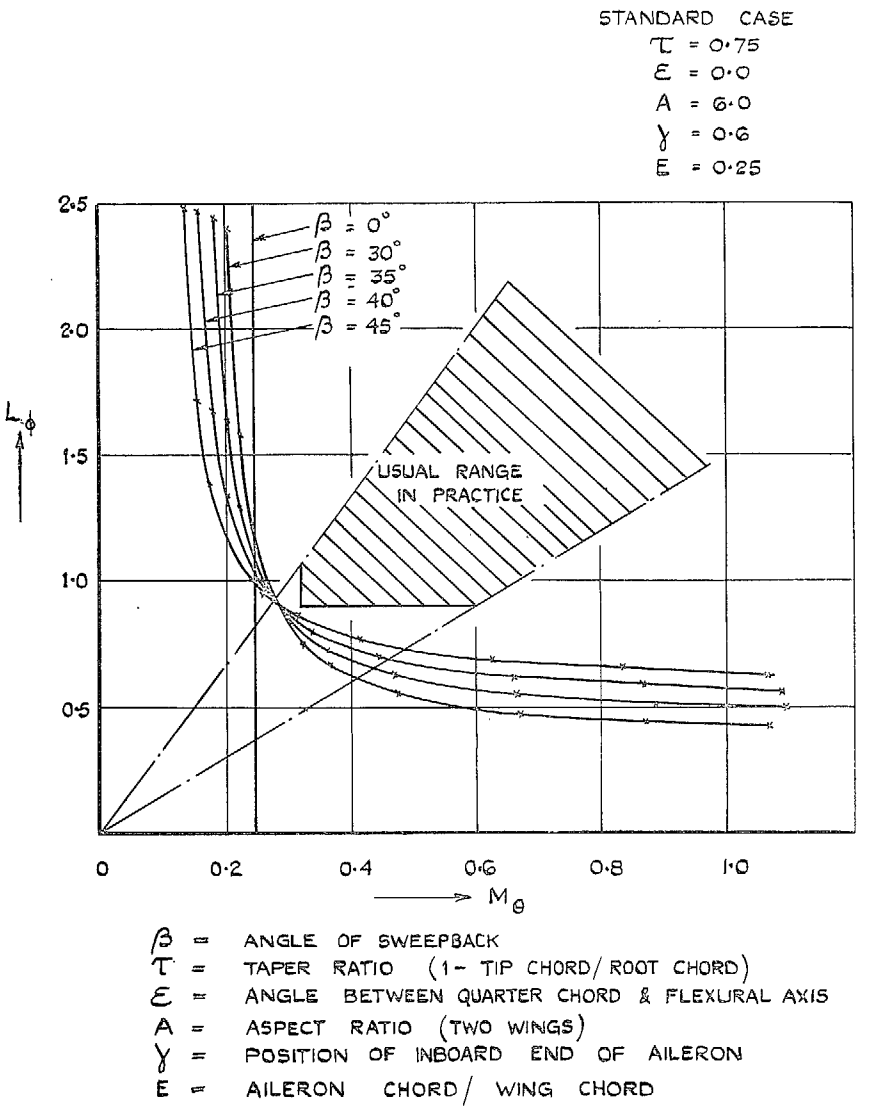

FIG. 2. Variation of aileron reversal speed with wing stiffness. Standard wing.

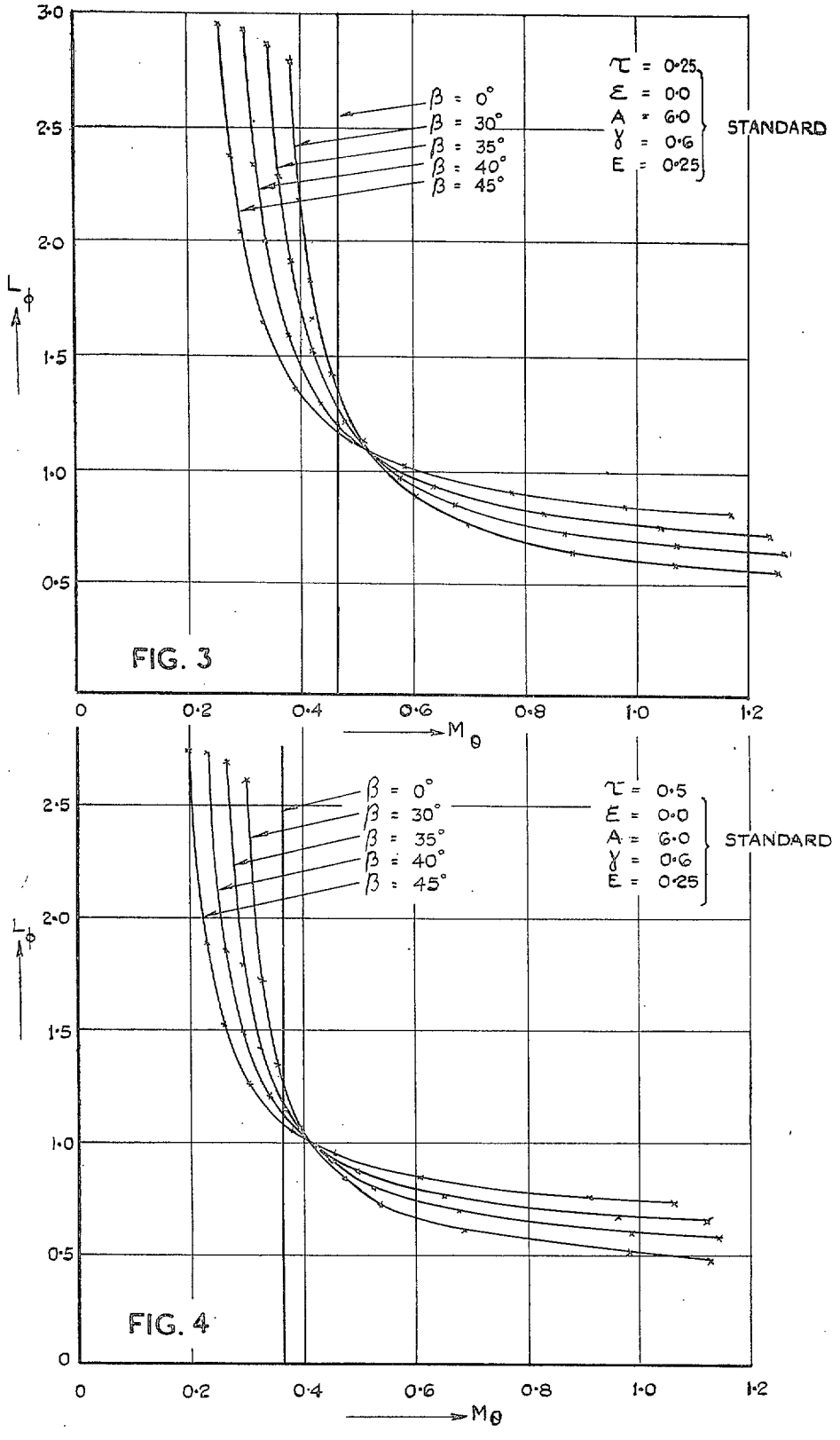

FIGS. 3 and 4. Variation of aileron reversal speed with wing stiffness. Effect of wing taper.

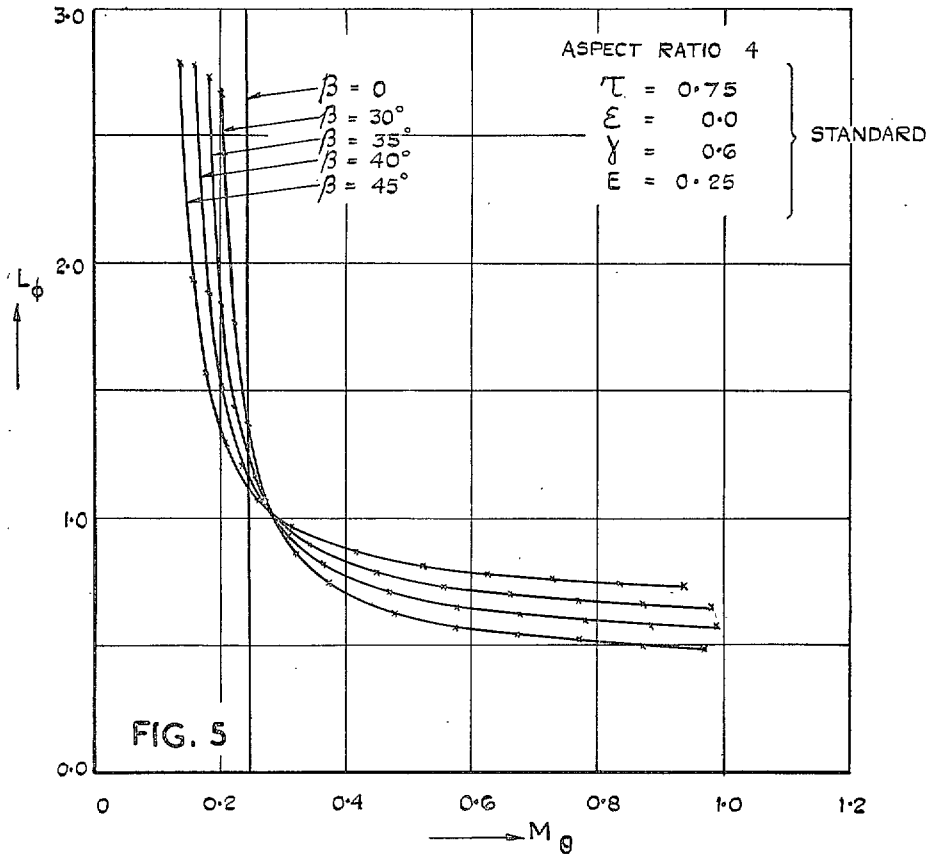

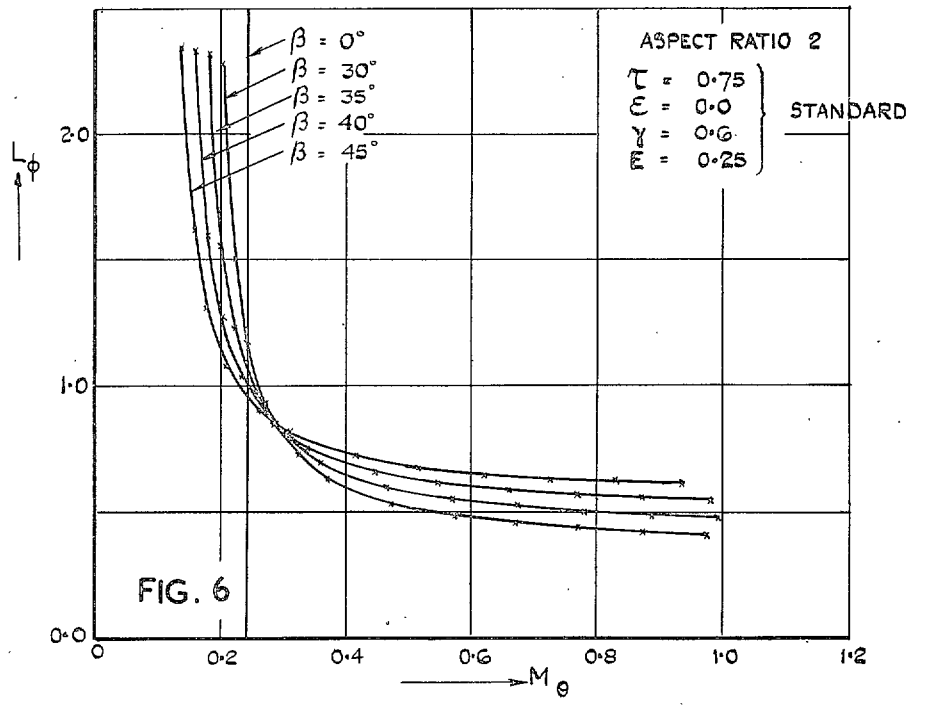

FIGS. 5 and 6. Variation of aileron reversal speed with wing stiffness. Effect of wing aspect ratio.

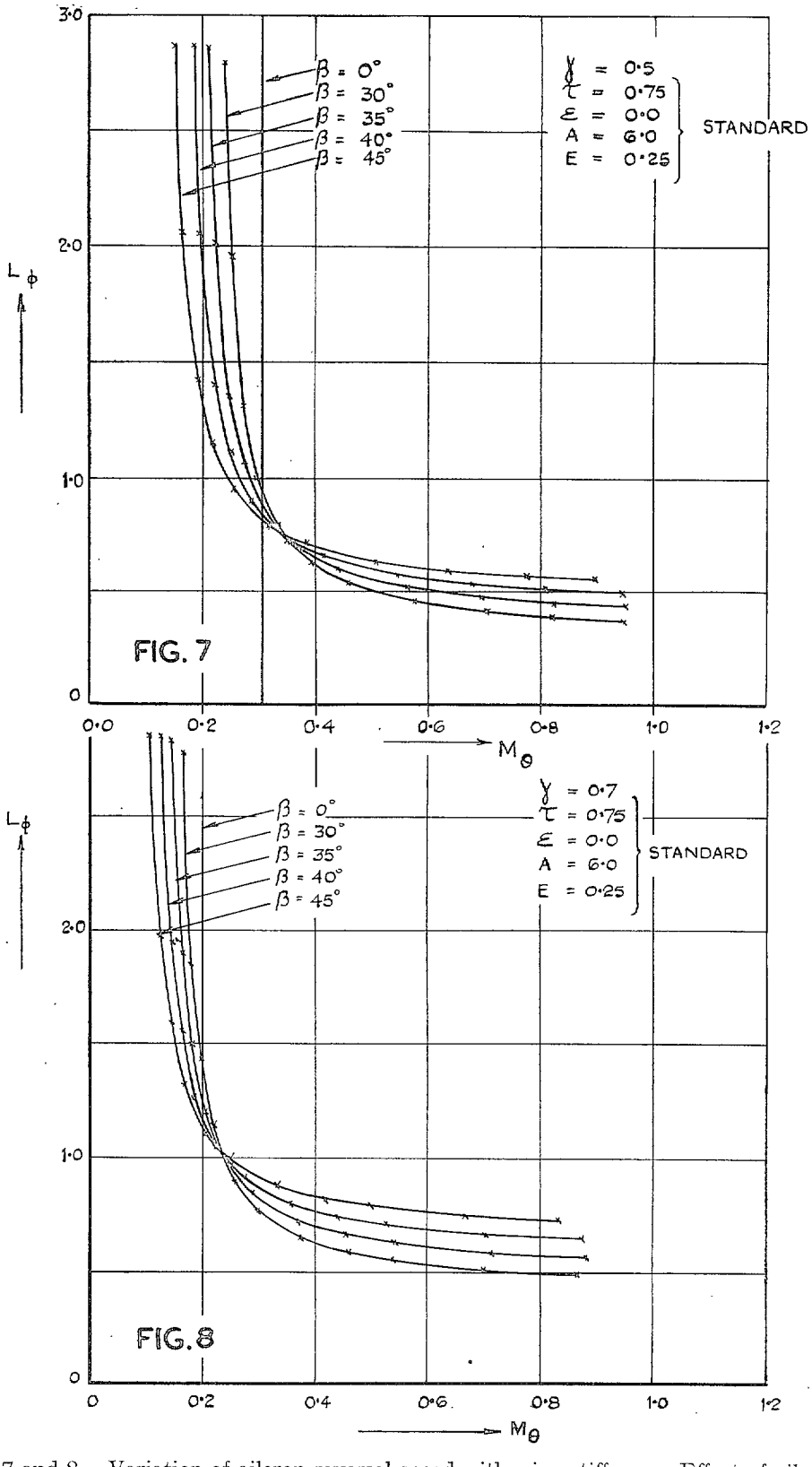

FIGS. 7 and 8. Variation of aileron reversal speed with wing stiffness. Effect of aileron span.

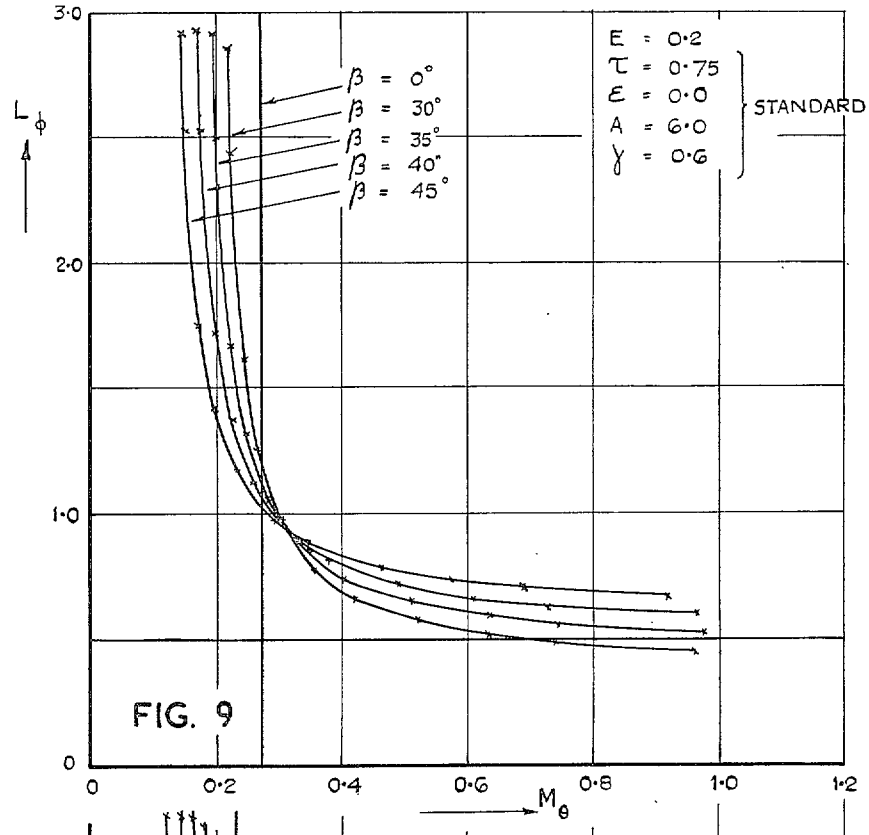

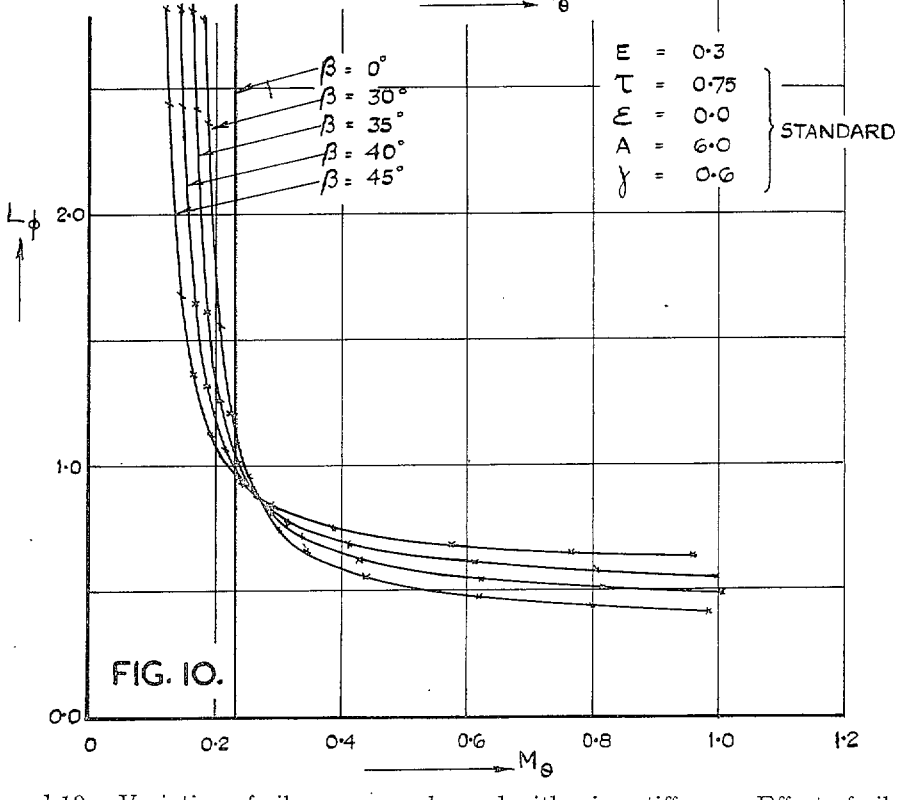

FIGS. 9 and 10. Variation of aileron reversal speed with wing stiffness. Effect of aileron chord.

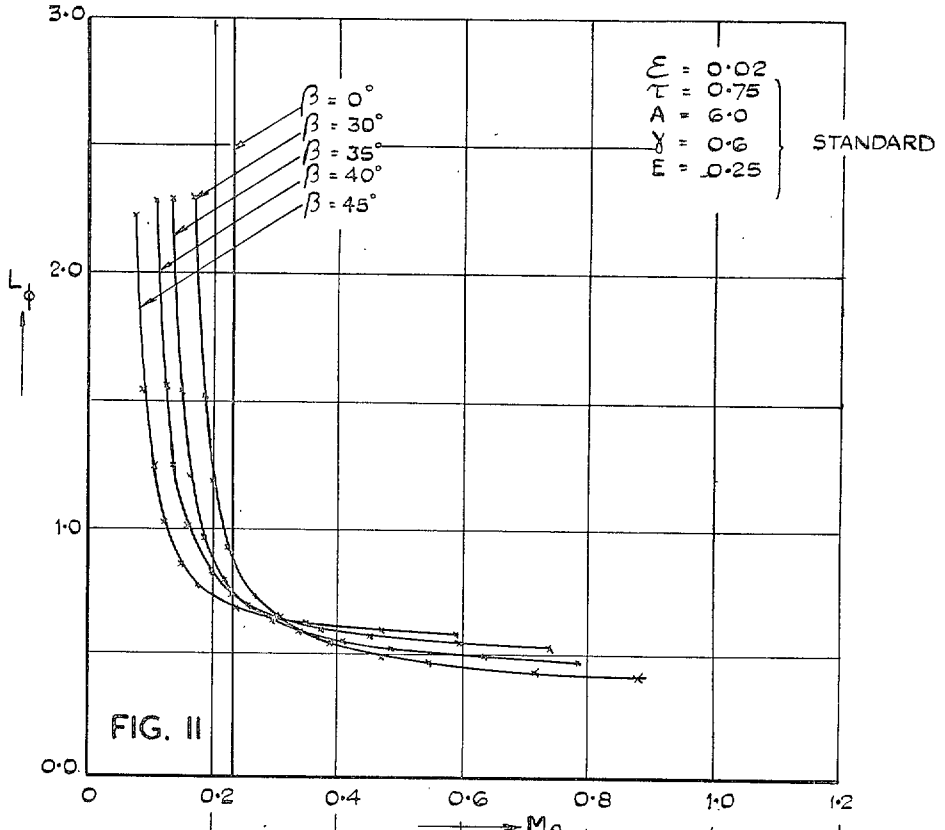

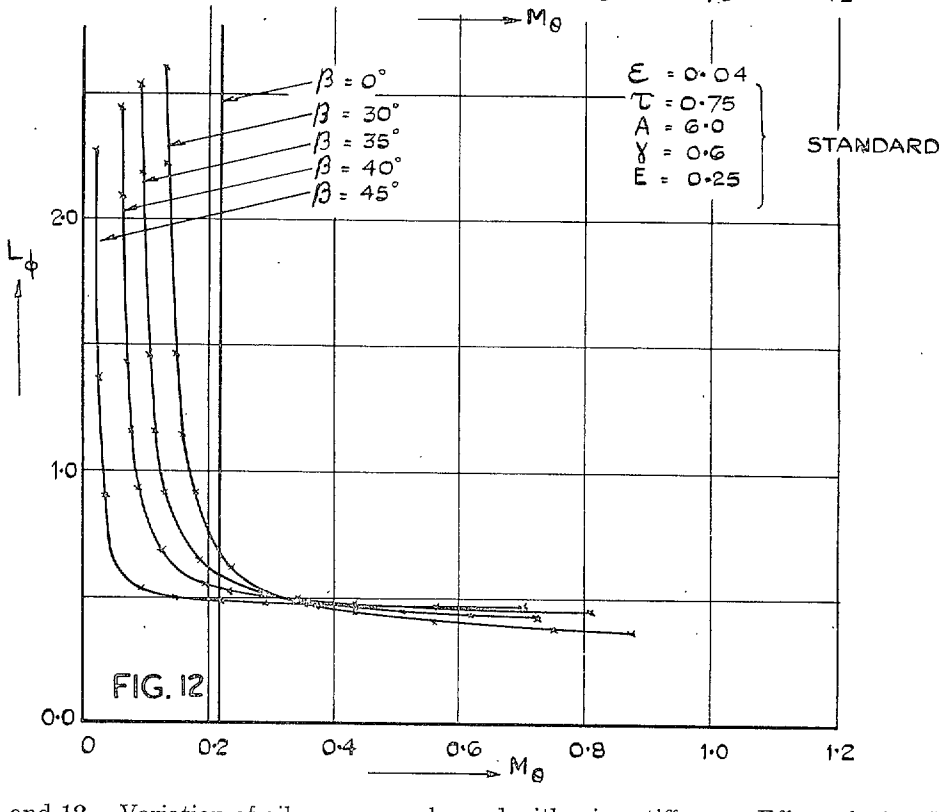

FIGS. 11 and 12. Variation of aileron reversal speed with wing stiffness. Effect of wing flexural axis.

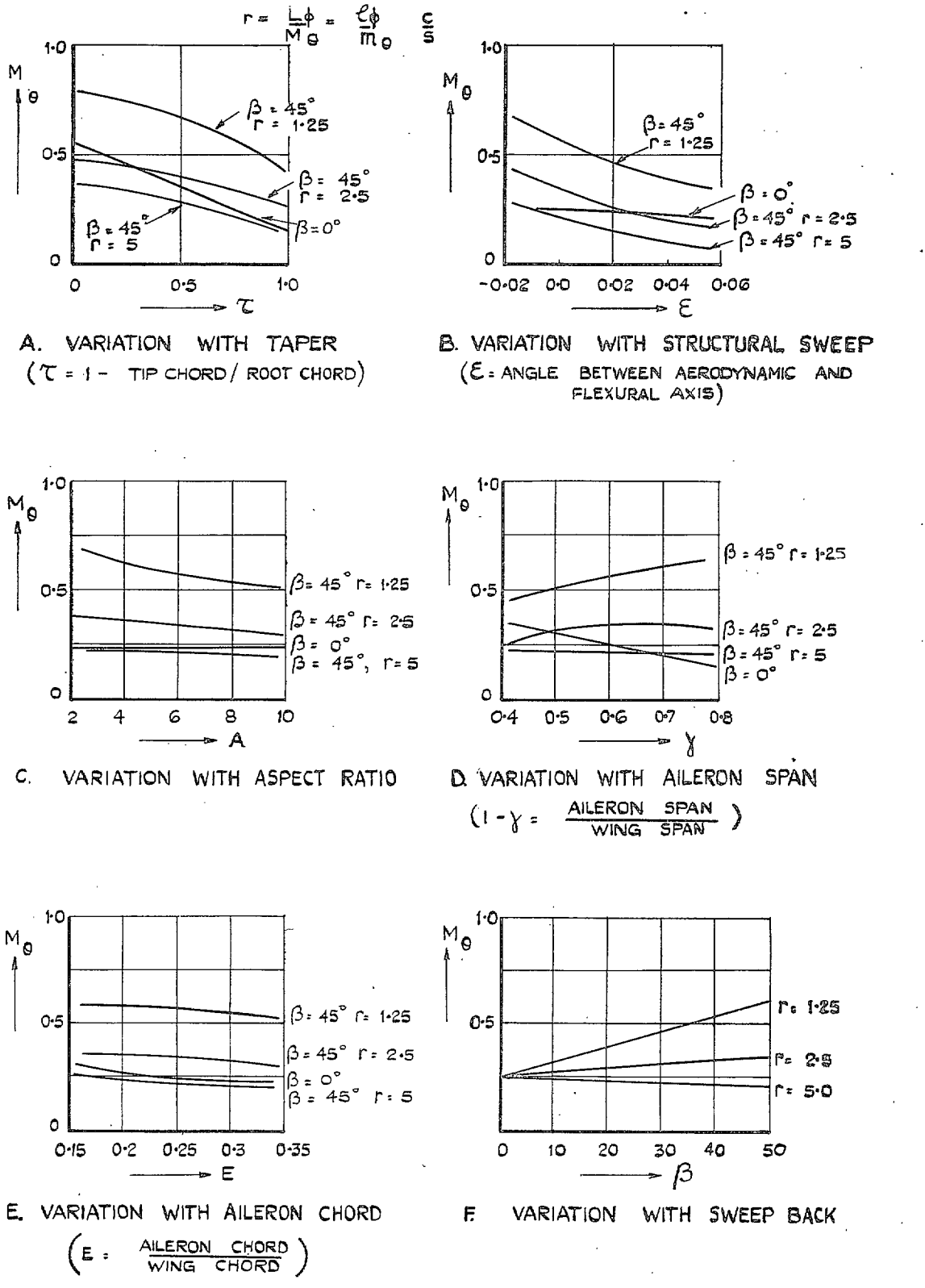

FIG. 13. Variation of wing torsional stiffness parameter with wing and aileron geometrical parameters.

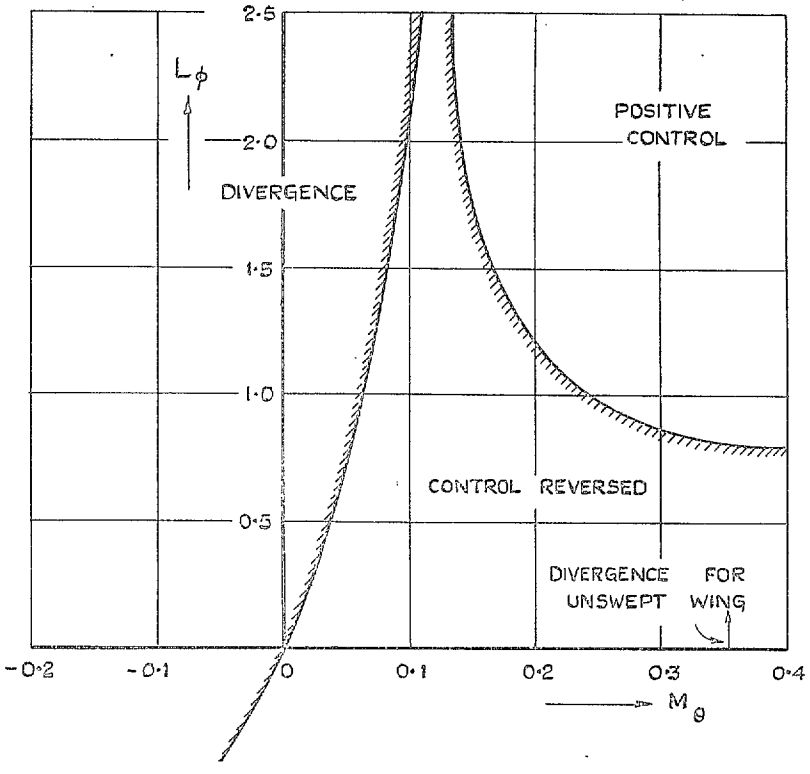

FIG. 14 Reversal and divergence diagram for flexural axis at 45 per cent chord with 45 deg sweepback. (The curves are shaded on the danger side.)

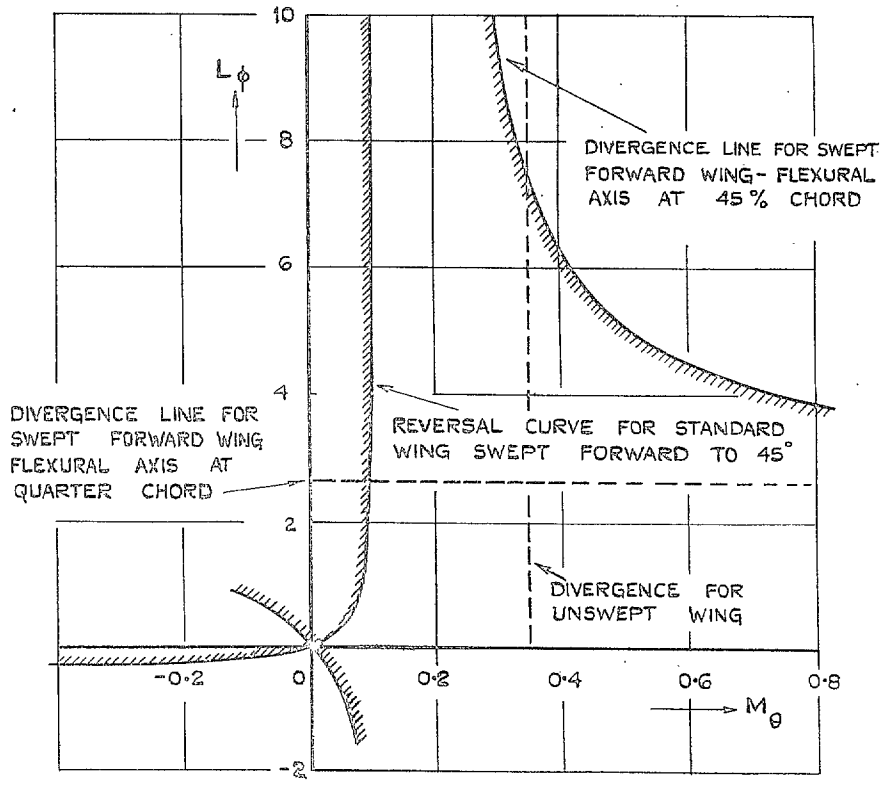

FIG. 15. Stiffness diagram for a wing swept forward at 45 deg. (The curves are shaded on the danger side.)

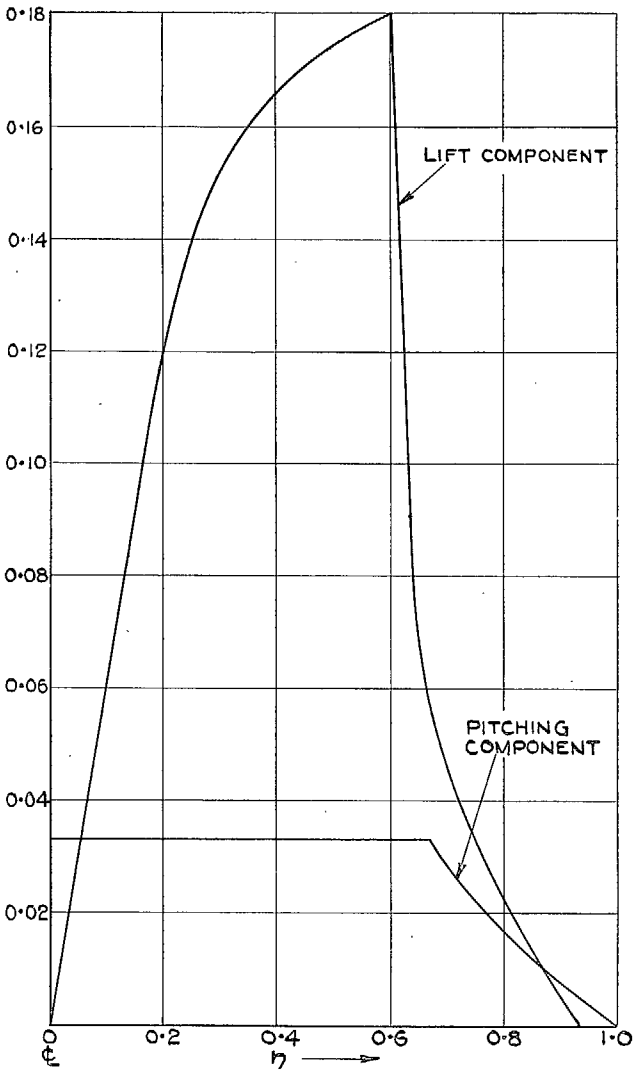

FIG. 16. Relative magnitudes of lifting and pitching components on the bending moment at a section η.

(Torsional stiffness infinite.)

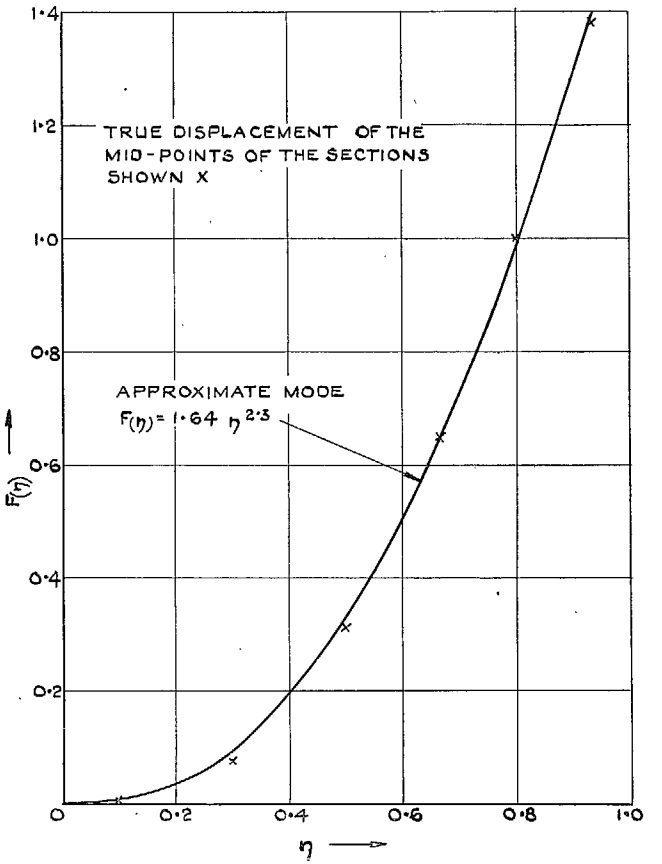

FIG. 17. Comparison of flexural mode with approximate analytical mode.

(Torsional stiffness infinite.)

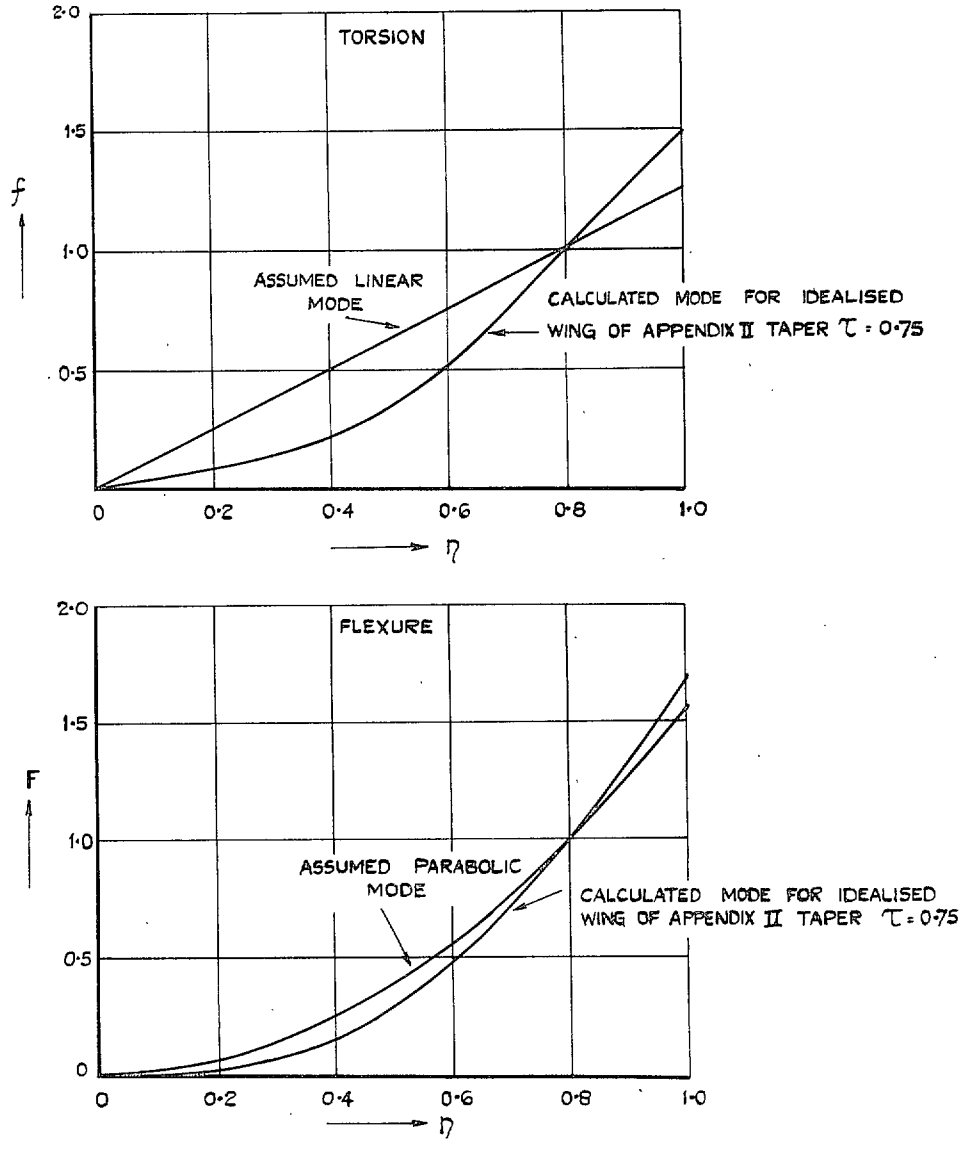

FIG. 18 A check on the shape of the assumed modes for a particular extreme case. The idealised wing of Appendix II.

J4296 Wt.17/680 K9 4/54 D&Co. 34/263 PRINTED IN GREAT BRITAIN

Publications of the Aeronautical Research Council

ANNUAL TECHNICAL REPORTS OF THE AERONAUTICAL RESEARCH COUNCIL (BOUND VOLUMES)

1936 Vol. I. Aerodynamics General, Performance, Airscrews, Flutter and Spinning. 40*s.* (40*s.* 9*d.*)

Vol. II. Stability and Control, Structures, Seaplanes, Engines, etc. 50*s.* (50*s.* 10*d.*)

1937 Vol. I. Aerodynamics General, Performance, Airscrews, Flutter and Spinning. 40*s.* (40*s.* 10*d.*)

Vol. II. Stability and Control, Structures, Seaplanes, Engines, etc. 60*s.* (61*s.*)

1938 Vol. I. Aerodynamics General, Performance, Airscrews. 50*s.* (51*s.*)

Vol. II. Stability and Control, Flutter, Structures, Seaplanes, Wind Tunnels, Materials. 30*s.* (30*s.* 9*d.*)

1939 Vol. I. Aerodynamics General, Performance, Airscrews, Engines. 50*s.* (50*s.* 11*d.*)

Vol. II. Stability and Control, Flutter and Vibration, Instruments, Structures, Seaplanes, etc. 63*s.* (64*s.* 2*d.*)

1940 Aero and Hydrodynamics, Aerofoils, Airscrews, Engines, Flutter, Icing, Stability and Control, Structures, and a miscellaneous section. 50*s.* (51*s.*)

1941 Aero and Hydrodynamics, Aerofoils, Airscrews, Engines, Flutter, Stability and Control, Structures. 63*s.* (64*s.* 2*d.*)

1942 Vol. I. Aero and Hydrodynamics, Aerofoils, Airscrews, Engines. 75*s.* (76*s.* 3*d.*)

Vol. II. Noise, Parachutes, Stability and Control, Structures, Vibration, Wind Tunnels. 47*s.* 6*d.* (48*s.* 5*d.*)

1943 Vol. I. (*In the press.*)

Vol. II. (*In the press.*)

ANNUAL REPORTS OF THE AERONAUTICAL RESEARCH COUNCIL—

1933–34	1*s.* 6*d.* (1*s.* 8*d.*)	1937	2*s.* (2*s.* 2*d.*)
1934–35	1*s.* 6*d.* (1*s.* 8*d.*)	1938	1*s.* 6*d.* (1*s.* 8*d.*)
April 1, 1935 to Dec. 31, 1936.	4*s.* (4*s.* 4*d.*)	1939–48	3*s.* (3*s.* 2*d.*)

INDEX TO ALL REPORTS AND MEMORANDA PUBLISHED IN THE ANNUAL TECHNICAL REPORTS, AND SEPARATELY—

April, 1950 – – – – R. & M. No. 2600. 2*s.* 6*d.* (2*s.* 7½*d.*)

AUTHOR INDEX TO ALL REPORTS AND MEMORANDA OF THE AERONAUTICAL RESEARCH COUNCIL—

1909–1949 – – – – – R. & M. No. 2570. 15*s.* (15*s.* 3*d.*)

INDEXES TO THE TECHNICAL REPORTS OF THE AERONAUTICAL RESEARCH COUNCIL—

December 1, 1936 — June 30, 1939.	R. & M. No. 1850.	1*s.* 3*d.* (1*s.* 4½*d.*)
July 1, 1939 — June 30, 1945.	R. & M. No. 1950.	1*s.* (1*s.* 1½*d.*)
July 1, 1945 — June 30, 1946.	R. & M. No. 2050.	1*s.* (1*s.* 1½*d.*)
July 1, 1946 — December 31, 1946.	R. & M. No. 2150.	1*s.* 3*d.* (1*s.* 4½*d.*)
January 1, 1947 — June 30, 1947.	R. & M. No. 2250.	1*s.* 3*d.* (1*s.* 4½*d.*)
July, 1951 – – – –	R. & M. No. 2350.	1*s.* 9*d.* (1*s.* 10½*d.*)

Prices in brackets include postage.

Obtainable from

HER MAJESTY'S STATIONERY OFFICE

York House, Kingsway, London W.C.2 ; 423 Oxford Street, London W.1 (Post Orders : P.O. Box No. 569, London S.E.1) ; 13A Castle Street, Edinburgh 2 ; 39 King Street, Manchester 2 ; 2 Edmund Street, Birmingham 3 ; 1 St. Andrew's Crescent, Cardiff ; Tower Lane, Bristol 1 ; 80 Chichester Street, Belfast OR THROUGH ANY BOOKSELLER

S.O. Code No. 23-2817